Inorganic Chemistry

Article

pubs.acs.org/IC

Investigation of Thorium Salts As Candidate Materials for Direct Observation of the ^{229m}Th Nuclear Transition

Jason K. Ellis, Xiao-Dong Wen, and Richard L. Martin*

Theoretical Division, Los Alamos National Laboratory, Los Alamos, New Mexico 87545, United States

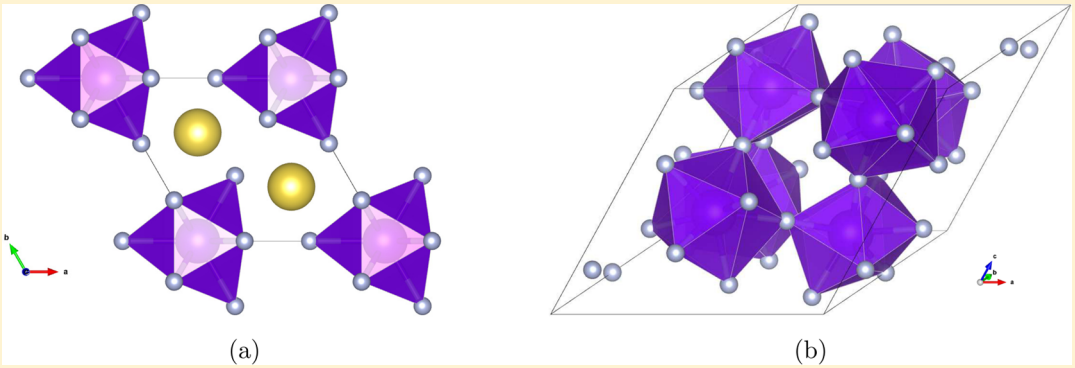

ABSTRACT: Recent efforts to measure the ^{229m}Th → ^{229g}Th nuclear transition sparked interest in understanding the electronic structure of wide-gap thorium salts. Such materials could be used to measure this nuclear transition using optical spectroscopy in solid-state devices. Here, we present screened hybrid density functional theory and many-body G_0W_0 calculations of two candidate materials, namely, Na_2ThF_6 and ThF_4, for such a measurement. Our results show an electronic gap larger than 10 eV for both materials, suggesting that the internal conversion nuclear de-excitation channel would be suppressed in these materials. We also present results for ThX_4 (X = Cl, Br, I), materials with smaller gaps significantly easier to access experimentally.

INTRODUCTION

A more accurate time reference will significantly impact a variety of fields, from general relativity to experimental constraints on the values of fundamental constants. This motivates several recent efforts toward building next-generation atomic clocks. Decoupling the oscillator (typically an atomic transition) from the environment remains a challenge for current clock designs. These systems require complicated schemes such as atomic fountains or optical lattices to reduce environmental influences. Recently several proposals came forward to build an optical clock based on a nuclear, rather than atomic transition.[1−3] Such a clock would be significantly less sensitive to the environment due to screening by the atomic electrons.[4] In particular, indirect measurements infer that the metastable isomeric state ($I = 3/2^+$) of ^{229}Th lies 7.6 ± 0.5 eV above the ground state ($I = 5/2^+$).[5] Though this transition lies in the vacuum ultraviolet (VUV) spectrum, it remains, in principle, accessible via laser spectroscopy. Direct measurement of this metastable state would be the first step toward building an optical clock based on this nuclear transition.

One proposal for measuring this transition involves using a VUV light source to interrogate a large number of ^{229}Th nuclei. By doping ^{229}Th into a wide band gap solid-state crystal, densities as high as 10^{19} nuclei/cm^3 may be obtained, far outstripping the 10^8 nuclei/cm^3 obtainable using laser-cooled atomic traps.[3] This isomeric metastable nuclear state may decay in two ways: by emission of a VUV photon (which we will loosely refer to as a γ-ray to denote its origin in a nuclear transition), or by the emission of an electron from the electronic states available to the atom and its environment. We will refer to the latter as the internal-conversion channel. Blocking the internal-conversion channel maximizes the probability of optical decay. If the band gap of the host crystal lies higher in energy than the ∼7.6 eV nuclear transition, then conservation of energy considerations forbid nuclear decay via the internal conversion channel. Consequently, our work focused on screening candidate materials with gaps greater than ∼7.6 eV. We investigated the electronic structure of two stochiometric candidate materials, ThF_4 and Na_2ThF_6, using both hybrid density functional theory[6,7] (DFT) as well as the GW many-body approach[8] to assess their suitability for such experiments. In addition, we studied the larger halides in the ThX_4 (X = F, Cl, Br, I) family of materials.

COMPUTATIONAL METHODS

We sought to establish the suitability of the candidate materials Na_2ThF_6 and ThF_4 for use in measuring the ^{229m}Th nuclear transition. Screened hybrid functionals, such as Heyd−Scuseria−Ernzerhof (HSE), show significant improvement over local density approximation (LDA) and generalized gradient approximation (GGA) functionals for materials with moderate band gaps (<5−6 eV).[7,9] In fact, they yield reliable gaps even for strongly correlated actinide oxides.[10,11] However, recent calculations indicate that HSE systemati-

Received: March 12, 2014
Published: June 17, 2014

dx.doi.org/10.1021/ic500570u | Inorg. Chem. 2014, 53, 6769−6774

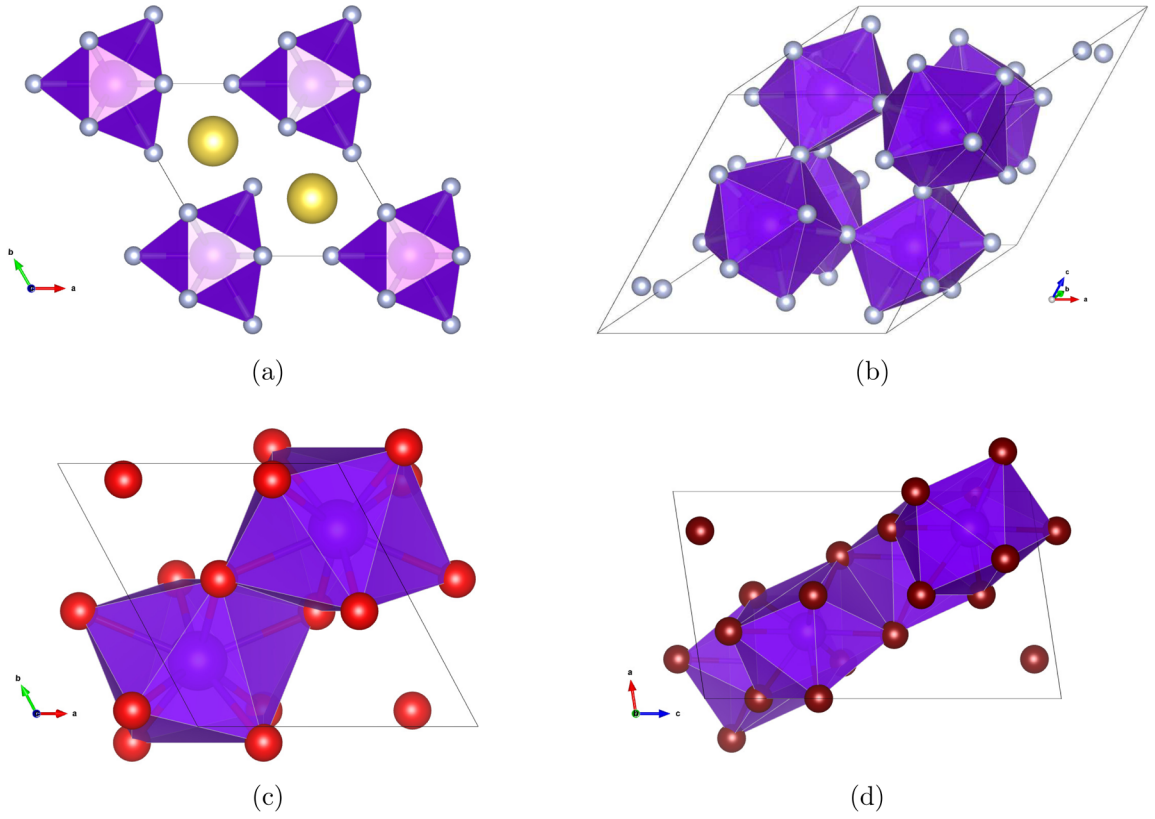

Figure 1. Crystal structures for (a) Na_2ThF_6, (b) ThF_4, (c) $ThBr_4$, and (d) ThI_4. The crystal structure for $ThCl_4$ is similar to that of $ThBr_4$, differing only in the lengths of the lattice vectors.

Table 1. Parameters Used for G_0W_0 Calculations in This Work

material	k-point mesh	NBANDS
ThI_4	3 × 2 × 2	648
$ThBr_4$	4 × 4 × 4	360
$ThCl_4$	3 × 3 × 3	360
ThF_4	3 × 2 × 2	960
Na_2ThF_6	5 × 4 × 4	224

cally underestimates band gaps for wide-gap (>6 eV) insulators.[12] The GW approximation,[8] an alternative to hybrid DFT, increases the computed gap relative to HSE for a number of wide band gap insulators.[12] This approximation also appears to systematically underestimate the experimental gap, with an error significantly decreased relative to HSE.

However, *f*-electron systems present an ongoing challenge for electronic structure methods and for the GW approximation in particular. Localized *f*-bands remain difficult to describe using this approach, and there remains considerable work to be done in this area. A few groups have explored this issue in the context of correlated *f*-electron metals, semimetals, and narrow gap insulators, as well as lanthanide oxides.[13−16] In the wide-gap f^0 insulators considered in this work the *f*-bands are empty, and at first glance there should be no issue associated with improperly accounted for Coulomb interactions. More work is needed to confirm this expectation. In particular, experimental measurements of these gaps in single-crystal samples would be quite welcome.

The calculations reported below include both hybrid DFT results as well as "single-shot" (nonself-consistent) calculations. We refer to the latter in this work as G_0W_0. We anticipate, on the basis of past experience with similar wide-gap insulators, that our best estimate will be provided by the G_0W_0 approximation and that the HSE result will lie below that of G_0W_0. Below, we show that for the optical properties, both HSE and G_0W_0 produce qualitatively similar pictures, with G_0W_0 predicting a wider band gap, as anticipated. This gives us confidence that any localization-related errors in the GW approach should only affect the magnitude of the gap.

Crystal structures[17−21] for Na_2ThF_6 and ThX_4 (X = F, Cl, Br, I) were obtained from the Inorganic Crystal Structure Database (ICSD),[22] and the primitive unit cell for each was computed using the PyMatGen toolset.[23] To orient the reader, these structures are shown in Figure 1. The β phases of Na_2ThF_6, $ThCl_4$, and $ThBr_4$ were considered in this work.

DFT calculations were performed on the primitive cells using the periodic boundary condition code[24−26] in the Gaussian suite of programs.[27] DFT calculations reported in this work use the LDA[28] and the HSE screened hybrid functional.[6,7] We compare our results to GGA calculations using the Perdew−Burke−Ernzerhof (PBE) functional[29,30] performed by the Materials Project.[23] All DFT results reported here use completely relaxed, rather than experimental, geometries. In all cases a pruned (99 590) Lebedev quadrature grid was used to calculate the exchange-correlation functional, and an 8 × 8 × 12 k-point mesh was used for the k-space integration. We used a convergence criterion of 10^{-7} for the density matrix. Basis sets optimized for use in solids were used for sodium[31] and fluorine.[32] For the larger halides, namely, Cl, Br, and I, large-core (N_{el} = 10, 28, and 46, respectively) relativistic effective core potentials were used in conjunction with their uncontracted valence basis sets.[33] For thorium, a small-core (N_{el} = 60) relativistic effective core potential[34] was used. Very diffuse functions (exponents < 0.1) in the basis sets for thorium and the larger halides were omitted to eliminate linear dependencies in the periodic boundary conditions (PBC) calculations.

Our G_0W_0 calculations used the Vienna Ab-Initio Simulation Package (VASP) code and the experimental geometries.[35,36] The quasi-particle self-energy was evaluated on top of the LDA. The nonself-consistent aspect of this calculation is known to yield slightly smaller band gaps than a self-consistent GW approach, but it is significantly less computationally demanding.[35] We used the LDA

dx.doi.org/10.1021/ic500570u | Inorg. Chem. 2014, 53, 6769−6774

Table 2. Lattice Parameters Calculated with Various Levels of Density Functional Theory

	Na_2ThF_6		ThF_4		$ThCl_4$	$ThBr_4$	ThI_4		
method	*a*	*c*	*a*	*c*	*c*	*c*	*a*	*b*	*c*
expt.[a]	5.99	3.84	8.57	8.54	7.07	7.46	7.77	8.23	13.59
LDA	5.82	3.79	8.47	8.47	7.02	7.42	7.71	8.03	13.03
PBE[b]	6.08	3.87	8.61	8.61	7.18	7.60	8.47	8.21	13.79
HSE	6.01	3.86	8.59	8.58	7.21	7.59	8.34	8.07	13.22

[a]Experimental data from references 17−21. [b]PBE data taken from reference 23.

projector augmented wave pseudopotentials distributed with VASP with a 400 eV energy cutoff for all calculations. In Table 1, we present the size of the Γ-centered k-point mesh and number of bands used for each material.

RESULTS

Our calculated lattice parameters (using DFT) compared to experimental crystallographic data appear in Table 2. We found excellent agreement between our calculations and experiment for all the materials except for ThI_4. For this material, the HSE functional provided the smallest absolute error averaged over all three lattice parameters. The layers of ThI_4 cross the *ac* plane, and we found significant errors in the *a* and *c* lattice parameters of this material. This error may be attributable to dispersion effects between layers, which we have not accounted for in our calculations.

Table 3. Calculated Band Gaps (in eV) Using Various Electronic Structure Methods

material	LDA	PBE[a]	HSE	G_0W_0
Na_2ThF_6	6.7	6.5	8.9	11.1
ThF_4	6.8	6.5	8.9	10.1
$ThCl_4$	3.6	3.7	5.4	7.0
$ThBr_4$	2.9	2.9	4.3	5.4
ThI_4	1.8	1.8	2.8	4.7

[a]PBE data taken from reference 23.

Table 3 presents our calculated band gaps. Band gaps computed with the LDA and PBE are presented for completeness. The HSE functional systematically increased the gap relative to the LDA as the size of the halide decreases. The G_0W_0 approximation yielded a gap that was on average 1.5 eV larger than that found using HSE for these materials. We found that HSE predicts a gap of 8.9 eV for both candidate materials, while G_0W_0 predicts 11.1 eV for Na_2ThF_6 and 10.1 eV for ThF_4. Note that both approximations result in band gaps significantly higher (>1 eV) than the best estimate of the nuclear transition energy. As we have good reason to believe that both HSE and G_0W_0 underestimate the actual band gap of the material, *it seems very probable that the internal-conversion channel should be closed in both fluoride candidates.*

In Figures 2 and 3 we compare the HSE and G_0W_0 partial density of states for the candidate materials Na_2ThF_6 and ThF_4. We found that both materials possess a ligand-to-metal charge-transfer (LMCT) gap, with transitions from the fluorine *p*-orbitals to empty states on the thorium atom. We also found that both the character and the symmetry of the gap differ between the two materials. The indirect gap of Na_2ThF_6 was $F_{2p} \rightarrow Th_{5f}$, whereas the direct gap (on the Γ point) of ThF_4 was $F_{2p} \rightarrow Th_{6d}$. We attributed this difference in the symmetry of the lowest state in the conduction band to the local environment of the thorium atom.

We observed that the crystal structure of ThF_4 permits a strong overlap between the thorium *6d* orbitals, resulting in a significant interaction depicted in Figure 4. This stabilized the (unoccupied) in-phase *6d*−*6d* orbital and caused it to lie below the *f*-band. In Na_2ThF_6 the local crystal field environment allowed for minimal overlap between the *6d* orbitals of adjacent

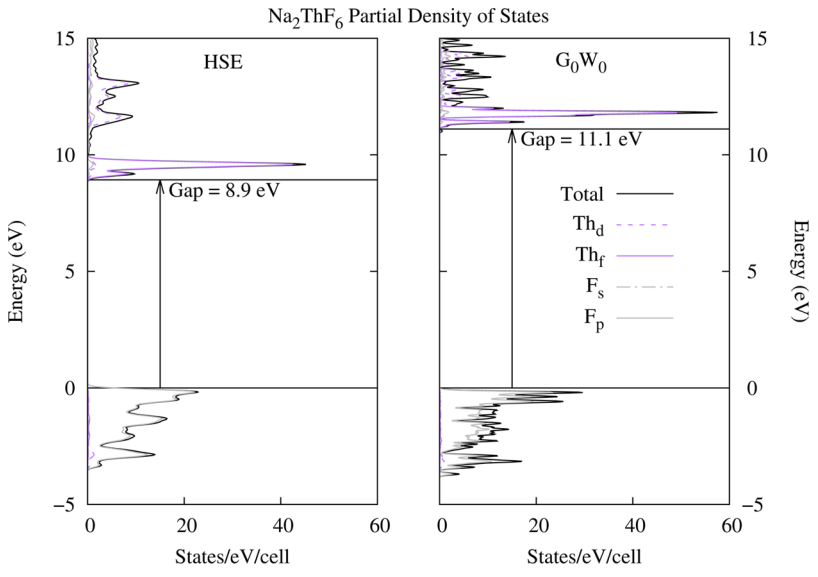

Figure 2. HSE and G_0W_0 partial density of states for Na_2ThF_6.

dx.doi.org/10.1021/ic500570u | Inorg. Chem. 2014, 53, 6769−6774

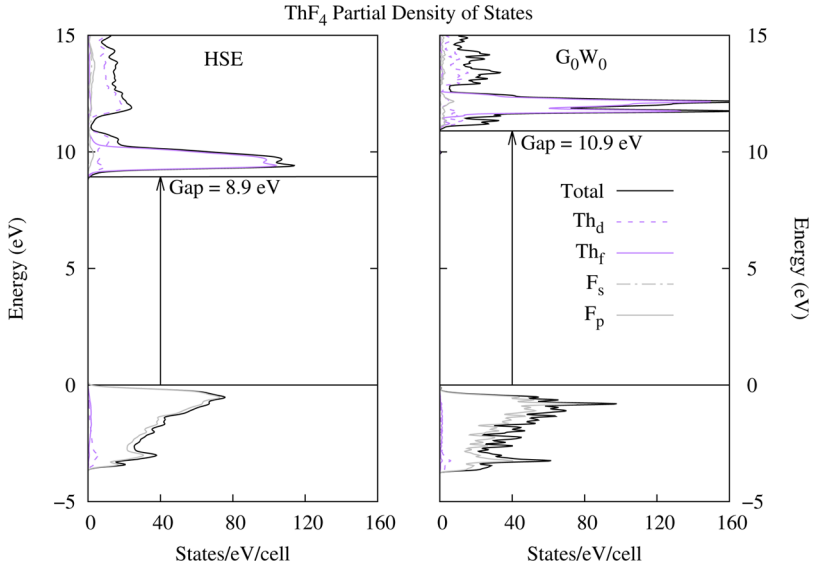

Figure 3. HSE and G_0W_0 partial density of states for ThF_4.

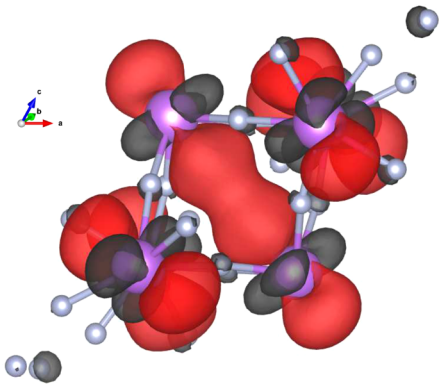

Figure 4. Lowest unoccupied crystal orbital of ThF_4, plotted at the Γ point. The overlap between the 6*d* orbitals stabilizes this band relative to the *f*-bands.

thorium atoms resulting in a clean separation between the *d*- and *f*-bands.

We also considered the larger halides (X = Cl, Br, I) of the ThX_4 family. As the size of the halide increased, we observed that the band gap decreased, and we found that none of the larger halides possessed a gap sufficiently large enough to close the internal conversion channel. This makes them less suitable candidate materials for measuring the ^{229m}Th nuclear transition by optical means. The HSE and G_0W_0 partial densities of states are plotted in Figures 5−7. Like ThF_4, we found that these materials all possessed a $X_p \rightarrow Th_{6d}$ LMCT gap. Two of these materials ($ThCl_4$ and $ThBr_4$) had indirect gaps, whereas ThI_4 was a direct-gap material. Both the chloride and bromide have tetragonal crystal structures (in contrast to the monoclinic structures of the fluoride and iodide). This resulted in significantly more splitting in the upper *d*-band compared to ThF_4 and ThI_4.

The nature of the lowest state in the conduction band of these materials (*f* vs *d*) remains a very subtle question worthy

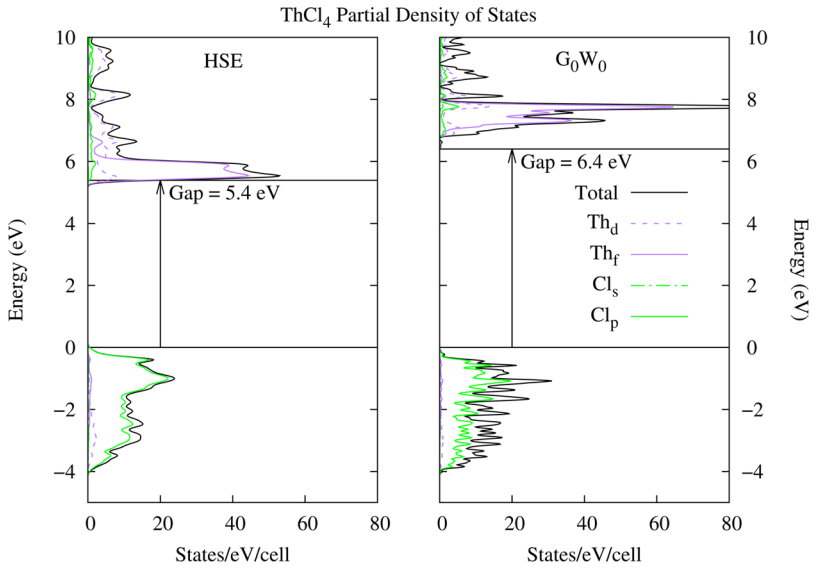

Figure 5. HSE and G_0W_0 partial density of states for $ThCl_4$.

dx.doi.org/10.1021/ic500570u | Inorg. Chem. 2014, 53, 6769−6774

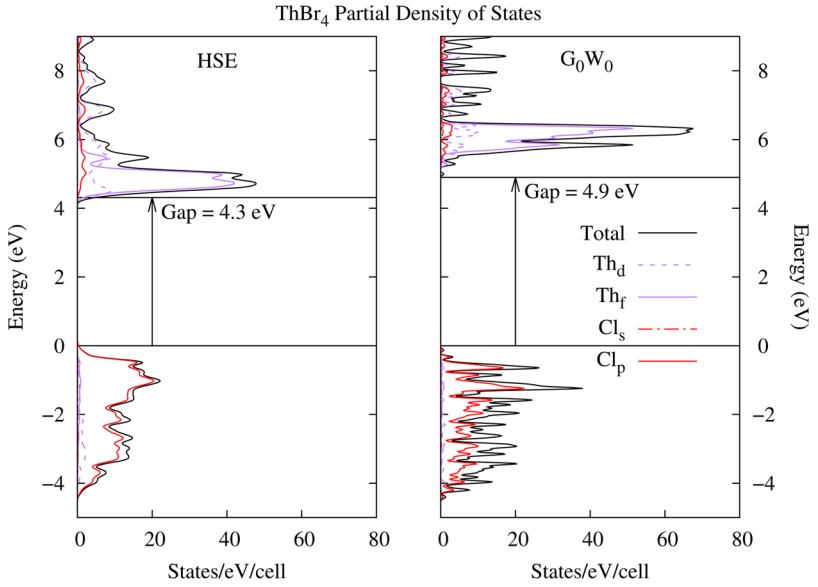

Figure 6. HSE and G_0W_0 partial density of states for $ThBr_4$.

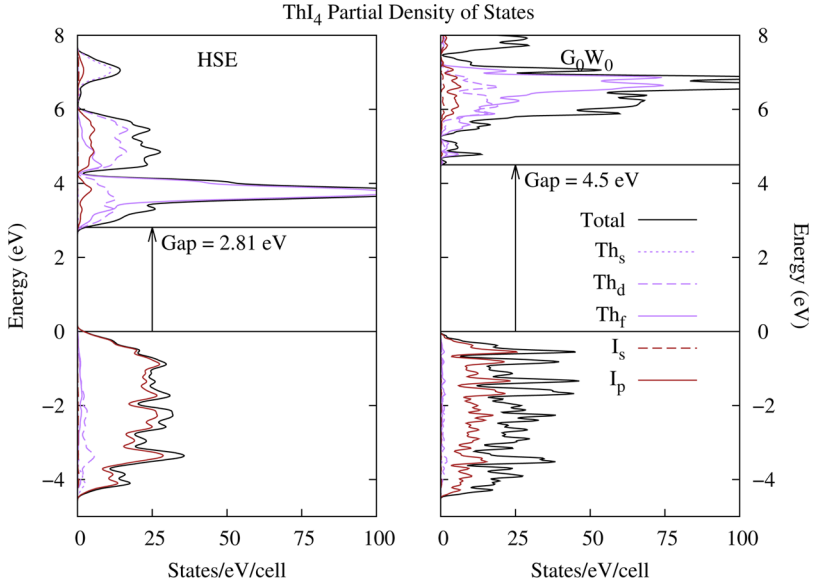

Figure 7. HSE and G_0W_0 partial density of states for ThI_4.

of further research. It will be of immediate import in determining the nature of the highest occupied orbital in related f^1 systems such as Th^{3+} or Pa. It may be possible to determine the symmetry of the states at the band edge using X-ray absorption spectroscopy. Such experiments might shed additional light on the theoretical results discussed here.

CONCLUSION

In summary, we presented screened hybrid DFT and G_0W_0 calculations of the electronic structure of several wide-gap thorium salts. Our HSE calculations establish a theoretical lower bound of 8.9 eV for the band gap of Na_2ThF_6 and ThF_4. The results from our G_0W_0 calculations predict a larger gap of 11.1 eV for Na_2ThF_6 compared to 10.1 eV for ThF_4. Both materials have gaps that are sufficiently separated from the ∼7.6 eV nuclear transition of ^{229}Th so as to suppress internal conversion, making them good candidate materials for experiment. For the larger halides of ThX_4 (X = Cl, Br, and I), we predicted band gaps of 6.4, 4.9, and 4.5 eV using the G_0W_0 method. In addition, we observed that the local symmetry around the thorium atom widely splits the *d*-bands in $ThCl_4$ and $ThBr_4$, whereas the strong overlap between the *d*-orbitals in ThI_4 drove them below the *f*-bands. X-ray absorption spectroscopy experiments may shed some light on the nature of the gap transition in these materials. In this work, we have not considered the presence of defects, impurities, or color centers that may contribute to the internal-conversion channel of the nuclear transition. Detailed analysis of these effects remains a work in progress.

AUTHOR INFORMATION

Corresponding Author

*E-mail: rlmartin@lanl.gov.

Notes

The authors declare no competing financial interest.

dx.doi.org/10.1021/ic500570u | *Inorg. Chem.* 2014, 53, 6769−6774

■ ACKNOWLEDGMENTS

This work was supported under the Heavy Element Chemistry Program at Los Alamos National Laboratory by the Division of Chemical Sciences, Geosciences, and Biosciences, Office of Basic Energy Sciences, U.S. Department of Energy. Portions of the work were also supported by the LDRD program at Los Alamos National Laboratory. J. E. and X.-D. W. gratefully acknowledge Seaborg Institute Fellowships. The Los Alamos National Laboratory is operated by Los Alamos National Security, LLC, for the National Nuclear Security Administration of the U.S. Department of Energy under Contract DE-AC5206NA25396. We thank Dr. X. Zhao for helpful discussions and suggestions for the manuscript.

■ REFERENCES

(1) Rellergert, W. G.; DeMille, D. P.; Greco, R. R.; Hehlen, M. P.; Torgerson, J. R.; Hudson, E. R. *Phys. Rev. Lett.* **2010**, *104*, 200802.
(2) Wense, L. v. d.; Thirolf, P. G.; Kalb, D.; Laatiaoui, M. *J. Instrum.* **2013**, *8*, P03005−P03005.
(3) Rellergert, W. G.; Sullivan, S. T.; DeMille, D. P.; Greco, R. R.; Hehlen, M. P.; Jackson, R. A.; Torgerson, J. R.; Hudson, E. R. *IOP Conf. Ser.: Mater. Sci. Eng.* **2010**, *15*, 2005.
(4) Hehlen, M. P.; Greco, R. R.; Rellergert, W. G.; Sullivan, S. T.; DeMille, D. P.; Jackson, R. A.; Hudson, E. R.; Torgerson, J. R. *J. Lumin.* **2013**, *133*, 91−95.
(5) Beck, B.; Becker, J.; Beiersdorfer, P.; Brown, G.; Moody, K.; Wilhelmy, J.; Porter, F.; Kilbourne, C.; Kelley, R. *Phys. Rev. Lett.* **2007**, *98*, 142501.
(6) Heyd, J.; Scuseria, G. E.; Ernzerhof, M. *J. Chem. Phys.* **2006**, *124*, 9906.
(7) Heyd, J.; Scuseria, G. E.; Ernzerhof, M. *J. Chem. Phys.* **2003**, *118*, 8207−8215.
(8) Hedin, L. *Phys. Rev.* **1965**, *139*, A796−A823.
(9) Heyd, J.; Peralta, J. E.; Scuseria, G. E.; Martin, R. L. *J. Chem. Phys.* **2005**, *123*, 174101.
(10) Wen, X.-D.; Martin, R. L.; Roy, L. E.; Scuseria, G. E.; Rudin, S. P.; Batista, E. R.; McCleskey, T. M.; Scott, B. L.; Bauer, E.; Joyce, J. J.; Durakiewicz, T. *J. Chem. Phys.* **2012**, *137*, 4707.
(11) Wen, X.-D.; Martin, R. L.; Henderson, T. M.; Scuseria, G. E. *Chem. Rev.* **2013**, *113*, 1063−1096.
(12) Chen, W.; Pasquarello, A. *Phys. Rev. B* **2012**, *86*, 035134.
(13) Chantis, A. N.; van Schilfgaarde, M.; Kotani, T. *Phys. Rev. B* **2007**, *76*, 165126.
(14) Jiang, H.; Gomez-Abal, R. I.; Rinke, P.; Scheffler, M. *Phys. Rev. Lett.* **2009**, *102*, 126403.
(15) Kutepov, A.; Haule, K.; Savrasov, S. Y.; Kotliar, G. *Phys. Rev. B* **2012**, *85*, 155129.
(16) Jiang, H.; Rinke, P.; Scheffler, M. *Phys. Rev. B* **2012**, *86*, 125115.
(17) Zachariasen, W. H. *Acta Crystallogr.* **1948**, *1*, 265−268.
(18) Benner, G.; Müller, B. G. *Z. Anorg. Allg. Chem.* **2004**, *588*, 33−42.
(19) Mason, J. T.; Jha, M. C.; Chiotti, P. *J. Less-Common Met.* **1974**, *34*, 143−151.
(20) Mason, J. T.; Jha, M. C.; Bailey, D. M.; Chiotti, P. *J. Less-Common Met.* **1974**, *35*, 331−338.
(21) Zalkin, A.; Forrester, J. D.; Templeton, D. H. *Inorg. Chem.* **1964**, *3*, 639−644.
(22) Belsky, A. N.; Hellenbrandt, M.; Karen, V. L.; Luksch, P. *Acta Crystallogr., Sect. B: Struct. Sci.* **2002**, *58*, 364−369.
(23) Jain, A.; Ong, S. P.; Hautier, G.; Chen, W.; Richards, W. D.; Dacek, S.; Cholia, S.; Gunter, D.; Skinner, D.; Ceder, G.; Persson, K. A. *APL Mater.* **2013**, *1*, 011002.
(24) Kudin, K. N.; Scuseria, G. E. *Phys. Rev. B* **2000**, *61*, 91200−16453.
(25) Kudin, K. N.; Scuseria, G. E. *Chem. Phys. Lett.* **1998**, *289*, 611−616.
(26) Kudin, K. N.; Scuseria, G. E. *Chem. Phys. Lett.* **1998**, *283*, 61−68.
(27) Frisch, M. J. et al. *Gaussian Development,* Version Revision H.11; Gaussian, Inc.: Wallingford, CT, 2010; http://www.gaussian.com/.
(28) Vosko, S. H.; Wilk, L.; Nusair, M. *Can. J. Phys.* **1980**, *58*, 1200−1211.
(29) Perdew, J. P.; Burke, K.; Ernzerhof, M. *Phys. Rev. Lett.* **1997**, *78*, 1396−1396.
(30) Perdew, J.; Burke, K.; Ernzerhof, M. *Phys. Rev. Lett.* **1996**, *77*, 3865−3868.
(31) Prencipe, M.; Zupan, A.; Dovesi, R.; Aprà, E.; Saunders, V. R. *Phys. Rev. B* **1995**, *51*, 3391−3396.
(32) Catti, M.; Pavese, A.; Dovesi, R.; Roetti, C.; Caus, M. *Phys. Rev. B* **1991**, *44*, 3509−3517.
(33) Bergner, A.; Dolg, M.; Küchle, W.; Stoll, H.; Preuss, H. *Mol. Phys.* **1993**, *80*, 1431−1441.
(34) Küchle, W.; Dolg, M.; Stoll, H.; Preuss, H. *J. Chem. Phys.* **1994**, *100*, 7535−7542.
(35) Shishkin, M.; Kresse, G. *Phys. Rev. B* **2007**, *75*, 235102.
(36) Shishkin, M.; Kresse, G. *Phys. Rev. B* **2006**, *74*, 035101.